Brain Pathology ISSN 1015-6305

RESEARCH ARTICLE

Reduced Glioma Growth Following Dexamethasone or Anti-Angiopoietin 2 Treatment

Jérôme Villeneuve; Hugo Galarneau; Marie-Josée Beaudet; Pierrot Tremblay; Ariel Chernomoretz*; Luc Vallières

Department of Oncology and Molecular Endocrinology, Laval University Hospital Research Center, Québec City, Québec, Canada.

Keywords
angiopoietin-2, antitumor immunity, gene profiling, glioblastoma, glucocorticoid, tumor endothelium.

Corresponding author:
Luc Vallières, Department of Oncology and Molecular Endocrinology, Laval University Hospital Research Center, 2705 Laurier Boulevard, T3-67, Québec City, Québec, G1V 4G2, Canada (E-mail: *Luc.Vallieres@crchul.ulaval.ca*)

Received 1 August 2007; accepted 3 December 2007.

* Current address: Departamento de Fisica, Facultad de Ciencias Exactas y Naturales, Universidad de Buenos Aires, Pabellon 1 Ciudad Universitaria, 1428, Buenos Aires, Argentina

doi:10.1111/j.1750-3639.2008.00139.x

Abstract

All patients with glioblastoma, the most aggressive and common form of brain cancer, develop cerebral edema. This complication is routinely treated with dexamethasone, a steroidal anti-inflammatory drug whose effects on brain tumors are not fully understood. Here we show that dexamethasone can reduce glioma growth in mice, even though it depletes infiltrating T cells with potential antitumor activity. More precisely, T cells with helper or cytotoxic function were sensitive to dexamethasone, but not those that were negative for the CD4 and CD8 molecules, including gammadelta and natural killer (NK) T cells. The antineoplastic effect of dexamethasone was indirect, as it did not meaningfully affect the growth and gene expression profile of glioma cells *in vitro*. In contrast, hundreds of dexamethasone-modulated genes, notably angiopoietin 2 (Angpt2), were identified in cultured cerebral endothelial cells by microarray analysis. The ability of dexamethasone to attenuate Angpt2 expression was confirmed *in vitro* and *in vivo*. Selective neutralization of Angpt2 using a peptide-Fc fusion protein reduced glioma growth and vascular enlargement to a greater extent than dexamethasone, without affecting T cell infiltration. In conclusion, this study suggests a mechanism by which dexamethasone can slow glioma growth, providing a new therapeutic target for malignant brain tumors.

INTRODUCTION

Brain tumors are a leading cause of cancer-related deaths in children and young adults (22). The most frequent and aggressive brain tumor, glioblastoma, carries a very poor prognosis, with a median survival of about 1 year, despite radical treatments, including surgical resection, irradiation and chemotherapy (33, 40). New, more targeted approaches, such as immunotherapy, anti-angiogenic therapy and gene therapy, have shown promise in experimental models, but their effectiveness in clinical settings remains to be proven (10, 16, 32, 33).

Vascular edema is a serious complication of brain tumors (45). It results from the disruption of the blood–brain barrier, allowing plasma to enter the interstitial space (31). Because this condition can cause neurological deficits and death, patients with brain tumors are treated with dexamethasone (23), a synthetic glucocorticoid with potent anti-inflammatory activity. Although this drug has been routinely used for decades in the management of cerebral edema, its precise mechanism of action is still poorly understood, but is thought to result in a reduction in the permeability of tumor capillaries and/or an increase in the clearance of extracellular fluid. Despite its usefulness, dexamethasone can produce many side effects, including Cushing's syndrome, myopathy and opportunistic infections (48). Furthermore, recent studies suggest that dexamethasone can potentially interfere with current and prospective anticancer treatments. For example, it has been shown that dexamethasone protects glioma cells from the chemotherapeutic agent temozolomide (6, 41), reduces the bystander effect of the thymidine kinase/ganciclovir system in suicide-gene therapy (35) and inhibits the antitumor effect of interleukin-4 when delivered using retroviruses (2).

Brain tumors are infiltrated by immune cells with potential antitumor activity (e.g. macrophages, T lymphocytes). Despite their presence in large numbers, these cells are normally unable to eradicate malignant tumors, but some evidence suggests that they can slow tumor progression to some extent. For example, we have shown in mice that glioma-associated macrophages, by expressing tumor necrosis factor, promote their own recruitment and reduce glioma growth through a process that culminates in the formation of microcysts (47). We have also shown that glioma growth is increased in mice depleted of macrophages (17). The exact mechanism by which macrophages can attack glioma cells is unclear,

but possibly involves contact-dependent interactions, secretion of cytotoxic and cytostatic factors, and/or recruitment of effector T cells. The ability of the latter to reduce glioma growth is suggested by an early clinical study that found an association between the presence of tumor-infiltrating lymphocytes and longer survival (3). More recently, it has been reported that the production levels of cytotoxic T cells by the thymus inversely correlates with tumor recurrence and mortality in glioblastoma patients and accounts for the effect of age on their prognosis, suggesting that T cells exert one of the strongest known influences on glioblastoma progression (49).

Considering that glucocorticoids can suppress cytokine signaling and induce T cell apoptosis (1, 7), the question arises as to whether dexamethasone may facilitate brain tumor growth by interfering with antitumor immune responses. In this study, we have tested this hypothesis and report that dexamethasone can, on the contrary, slow glioma growth, even though it depletes infiltrating T cells. Through the combined use of *in vitro* and *in vivo* techniques, we provide evidence that dexamethasone exerts this antitumor effect by acting on the tumor endothelium through a mechanism involving down-regulation of the angiogenic factor Angpt2.

METHODS

Intracerebral implantation of glioma cells

Eight-week-old male C57BL/6 mice (Charles River Laboratories, Montréal, Québec, Canada) were anesthetized, shaved and immobilized in a stereotaxic frame. A midline incision was made on the scalp, followed by a circular craniotomy over the right hemisphere, 1.7 mm lateral and 1 mm rostral from bregma. After removal of the dura mater, a 5-µL Hamilton syringe fitted with a 27-gauge beveled needle was advanced into the caudoputamen at a depth of 3.5 mm from the skull surface. Using a UMPII micropump (World Precision Instruments, Saratoga, FL, USA), 2 µL of Dulbecco's phosphate-buffered saline (DPBS; Invitrogen, Carlsbad, CA, USA) containing 5×10^4 viable GL261 cells were injected over 2 minutes. After injection, the syringe was left in place for 2 minutes before being withdrawn very slowly. All procedures were performed in accordance with current guidelines of the Canadian Council on Animal Care.

Dexamethasone treatment

From the day of tumor implantation to the day of death, mice were injected intraperitoneally twice daily with 0.1 or 1.0 mg/kg dexamethasone phosphate (Sabex, Boucherville, Québec, Canada) diluted in saline. Control mice were treated identically, except that dexamethasone was substituted by saline. As a point of comparison, the initial dose range used to treat peritumoral brain edema in humans is 4–16 mg/day; if insufficient, the dose can be increased up to 100 mg/day (48).

L1-10 treatment

From the day of tumor implantation to the day of death, mice were injected subcutaneously every other day with 4 mg/kg L1-10 (kindly provided by Amgen, Thousand Oaks, CA, USA) diluted in PBS. Control mice were treated identically, except that L1-10 was replaced by PBS.

Survival analysis

After tumor implantation, mice were monitored daily and killed when any of the following criteria were observed: >20% weight loss, paralysis or lethargy. Survival time was calculated from the day of tumor implantation to the day of euthanasia or death. The Kaplan–Meier method was used to create survival curves, which were compared using the log-rank test.

Flow cytometry

Twenty days after tumor implantation, mice were anesthetized and transcardially perfused with DPBS for 5 minutes. The tumors were dissected out, minced with razor blades in DPBS containing 2% goat serum, processed with the Medimachine™ (Dako, Carpinteria, CA, USA) and filtered through a 40-µm nylon mesh. Myelin debris was removed by centrifugation through 35% Percoll. Cells were rinsed, blocked for 5 minutes with 5 µg/mL anti-CD16/CD32 antibody (BD Biosciences, San Diego, CA, USA) and stained for 30 minutes on ice with combinations of the following rat antibodies (2 µg/mL each; all from BD Biosciences): CD11b-Alexa 488 (clone M1/70), CD3ε-Alexa 488 (clone 145-2C11), CD4-APC (clone RM4-5), CD4-PE (clone H129.19), CD8a-APC (clone 53-6.7), NK-1.1-PE (clone PK136), TCRβ-PE (clone H57-597) and TCRγδ-PE (clone GL3). Apoptotic cells (annexin V^+, propidium $iodide^-$) were labeled using the Vybrant® Apoptosis Assay Kit #2 (Molecular Probes, Eugene, OR, USA). Cells were analyzed using a two-laser, four-color FACSCalibur™ flow cytometer and CellQuest™ Pro software (BD Biosciences).

Histological preparation

For all histological analyses except *in situ* hybridization, mice were transcardially perfused with 10 mL of saline, followed by ice-cold 4% paraformaldehyde in phosphate buffer, pH 7.4, over 10 minutes. The brains were removed, postfixed for 4 h at 4°C then cryoprotected overnight in 50 mM potassium PBS supplemented with 20% sucrose. Series of sections through the tumors were cut at 40 µm using a freezing microtome, collected in cryoprotectant (30% ethylene glycol, 20% glycerol, 50 mM sodium phosphate buffer, pH 7.4) and stored at −20°C until analysis. For *in situ* hybridization, the following modifications were applied: (i) the fixative was dissolved in borate buffer, pH 9.5, instead of phosphate buffer; (ii) the brains were postfixed for 48 h before being cryoprotected overnight in the same fixative supplemented with 20% sucrose; and (iii) the tumors were cut at 30 µm.

Immunostaining

Immunohistochemistry was performed as described previously (47) using the following primary antibodies: rabbit anti-Iba1 (1:2000; Wako Chemicals, Richmond, VA, USA), rat anti-CD3ε (1:500; Serotec, Raleigh, NC, USA) and rat anti-CD31 (1:1000; BD Biosciences).

In situ hybridization

Transcripts were detected by radioisotopic *in situ* hybridization according to a previously described protocol (39). Briefly, sections were mounted onto Superfrost™ slides (Fisher Scientific, Pittsburgh, PA, USA), postfixed with 4% paraformaldehyde in borate buffer, pH 9.5, for 20 minutes, digested with 10 µg/mL proteinase K at 37°C for 25 minutes, acetylated with 0.25% acetic anhydride for 10 minutes and dehydrated. Antisense and sense cRNA probes were transcribed from linearized cDNAs (Table S1) in the presence of [^{35}S]-UTP and [^{35}S]-CTP (Perkin-Elmer, Foster City, CA, USA), purified by phenol–chloroform extraction and ammonium acetate–ethanol precipitation, then applied to the slides at a concentration of 2×10^7 cpm/mL in hybridization buffer (50% formamide, 0.3 M NaCl, 10 mM Tris, pH 8.0, 1 mM EDTA, 1 × Denhardt's solution, 10% dextran sulfate, 2 µg/mL tRNA and 10 mM dithiothreitol). After overnight incubation at 60°C, the slides were treated with 20 µg/mL ribonuclease A for 30 minutes at 37°C washed in a solution containing 15 mM NaCl and 1.5 mM sodium citrate for 30 minutes at 65°C and dehydrated. After film autoradiography, slides were defatted in xylene, dipped into Kodak NTB2 emulsion (Rochester, NY, USA), exposed at 4°C for 7 (Tnc, MMP2) or 14 (Angpt2, ESM1, TGFß2, VEGFa) days, developed in Kodak D19 developer for 3.5 minutes at 14–16°C fixed in Kodak rapid fixer for 5 minutes, counterstained with 0.25% thionin, dehydrated and coverslipped.

Quantitative histological analyses

For all analyses, systematically sampled sections (every 10th section through the tumors) were examined in a blind manner using a Stereo Investigator® system (Microbrightfield, Colchester, VT, USA) with a Nikon E800 microscope® (Nikon Canada, Mississauga, ON, Canada).

Tumor volume was estimated from thionin-stained sections by the Cavalieri method. Using a 2× Plan Apochromat® objective (numerical aperture 0.1), a point grid of 200 × 200 µm was overlaid on each section and the points that fell within the tumor were counted. The point counts were converted to volume estimates, taking into account sampling frequency, magnification, grid size and section thickness.

Immunolabeled cells were counted by the optical fractionator method. Tumor tissue was traced using a 2× objective and sampled using a 60× Plan Apochromat oil objective (numerical aperture 1.4). The counting parameters were as follows: distance between counting frames, 400 × 400 µm (Iba1$^+$ cells) or 450 × 450 µm (CD3ε$^+$ cells); counting frame size, 50 × 50 µm (Iba1$^+$ cells) or 100 × 100 µm (CD3ε$^+$ cells); disector height, 10 µm; guard zone thickness, ≥2 µm. The cells were counted only if their nucleus was within the disector area, did not intersect forbidden lines and came into the focus as the optical plane moved through the height of the disector.

Cells positive for *in situ* hybridization were counted using the fractionator method. Tumor tissue was traced using a 2× objective and sampled using a 40× Plan Apochromat objective (numerical aperture 0.95). The counting parameters were as follows: distance between counting frames, 400 × 400 µm; counting frame size, 150 × 150 µm. The hybridization signals (clusters of emulsion grains) were counted only if they were within the counting frame and did not intersect forbidden lines.

Tumor vessel density was evaluated from CD31-immunostained section by the area fraction fractionator method. Tumor tissue was traced using a 2× objective and sampled using a 40× Plan Apochromat oil objective (numerical aperture 0.95). The analysis parameters were as follows: counting frame size, 400 × 400 µm; distance between counting frames, 1000 × 1000 µm; grid size within counting frame, 35 × 35 µm. The numbers of points that fell on the vasculature and on the tumor in each counting frame were converted to area estimates, taking into account sampling frequency, magnification and grid size.

Tumor vessel caliber was measured using the Quick Measure Line tool of Stereo Investigator. For unbiased sampling, a point grid of 325 × 325 µm was overlaid on each section and the vessel diameter was recorded systematically where points fell on the vasculature.

In situ hybridization signals for Angpt2 were quantified at the single-cell level by optical densitometry. For unbiased sampling, all the tumor areas were photographed (12 bit, grayscale) in dark-field microscopy using a 20× Plan® objective (Nikon) and a Retiga™ EX monochrome camera (QImaging, Burnaby, British Columbia, Canada), and then one image out of three was used for quantification. The intensity of each hybridization signal on each image (100–150 per mouse) was analyzed with ImageJ software 1.36 (http://rsb.info.NIH.gov/ij). To this end, the signal was circled using the round selection tool of a fixed dimension (50 × 50 pixels) and the mean optical intensity of that area was recorded. The background from an average of six measurements was subtracted from the signal measured.

In situ hybridization signals for MMP2 were quantified by exposing the slides to PhosphorImager® screens (Molecular Dynamics, Sunnyvale, CA, USA) for 3 h, after which the screens were scanned using a Storm® 860 PhosphorImager (Molecular Dynamics). The tumor area on each section was traced with the freehand selection tool of ImageJ and the mean optical intensity of that area was recorded.

Imaging

Photomicrographs were taken using a Retiga EX monochrome camera mounted on a Nikon E800 microscope. The images were adjusted for contrast, brightness and sharpness using Photoshop® 7 (Adobe Systems, San Jose, CA, USA).

Cell culture and RNA preparation

The glioma cell line GL261, originally derived from a B6 mouse implanted intracerebrally with methylcholanthrene (38) and recently characterized (42), was provided by Dr. Protul Shrikant (Roswell Park Cancer Institute, Buffalo, NY, USA). The murine brain endothelial cell line bEnd.3 was obtained from American Type Culture Collection (Manassas, VA, USA). Cells were cultured in six-well plates for 24 h with Dulbecco's modified Eagle's medium (Wisent, Saint-Bruno, Québec, Canada) supplemented with 10% heat-inactivated fetal bovine serum, 2 mM L-glutamine, 110 mg/L sodium pyruvate, 100 U/mL penicillin and 100 µg/mL streptomycin. Thereafter, the medium was replaced with fresh medium supplemented or not with different concentrations of dexamethasone or L1-10. For cell growth assays, GL261 cells were seeded at 10 000 cells/well, collected by trypsinization 3 or 5 days

after drug addition and counted with an Epic® XL flow cytometer (Coulter, Miami, FL, USA) by excluding dead cells by propidium iodide staining. To estimate the proportion of cells in S phase of the cell cycle, cells were fixed for 30 minutes with 70% ethanol, stained for 30 minutes with a solution containing 50 µg/mL propidium iodide and 1.4 mg/mL RNase A, then analyzed by flow cytometry with Multicycle™ software (Phoenix Flow Systems, San Diego, CA, USA). The percentage of apoptotic cells was estimated by flow cytometry using the Vybrant Apoptosis Assay Kit #2 according to the manufacturer's protocol. For microarray and qRT-PCR analyses, cells were seeded at 50 000 (GL261) or 20 000 (dEnd.3) cells/well, and total RNA was extracted 24 h after stimulation using the GenElute™ Mammalian Total RNA Miniprep Kit (Sigma-Aldrich, St. Louis, MO, USA). RNA integrity and yield were assessed by microcapillary electrophoresis (Bioanalyzer 2100®, Agilent Technologies, Palo Alto, CA, USA).

Microarray analysis

RNA (12 ng) was converted to cDNA, which was amplified and transcribed to produce biotinylated cRNA using the Small Sample Labeling Protocol Version 2 (Affymetrix, Santa Clara, CA, USA). cRNA (15 µg) was fragmented and hybridized to Affymetrix GeneChip® Mouse Genome 430 2.0 arrays for 16 h at 45°C with constant rotation at 60 rpm. The arrays were washed and stained with streptavidin-phycoerythrin (10 µg/mL; Molecular Probes) and biotinylated goat anti-streptavidin (3 mg/mL; Vector Laboratories, Burlingame, CA, USA) using the Affymetrix GeneChip Fluidics Station 400 (protocol EukGE-WS2Av5), then read using the Affymetrix GeneChip Scanner 3000.

Microarray data were analyzed with the statistical software R (version 2.3.1; available from http://www.r-project.org) and add-on packages from the Bioconductor project (version 1.8; available from http://www.bioconductor.org). Briefly, after assessing array quality using the AffyPLM and AffyQCReport packages, the hybridization signals were background-corrected, normalized and summarized with the GCRMA package. To identify differentially expressed genes, empirical Bayes moderated *t*-statistics were computed with the LIMMA package, adjusting the corresponding *P*-values using the Benjamini and Hochberg's method to control the false discovery rate at 5%. Annotations were obtained from the Affymetrix web site. Genes were classified according to their molecular function using GeneSpring® GX version 7.3 (Silicon Genetics, Redwood City, CA, USA).

Real-time quantitative RT-PCR

RNA (1.25 µg) was reverse transcribed for 10 minutes at 25°C and for 120 minutes at 42°C using a random primer hexamer and Superscript™ II reverse transcriptase (Invitrogen). Quantitative PCR was conducted in duplicate in a final volume of 15 µL containing 1× Universal PCR Master Mix (Applied Biosystems, Foster City, CA, USA), 10 nM Z-tailed forward primer (Table S2), 100 nM untailed reverse primer (Table S2), 100 nM Amplifluor Uniprimer™ (Chemicon, Temecula, CA, USA) and 2 µL cDNA (40–50 ng/µL). Amplification was performed using the ABI PRISM® 7900 sequence detector (Applied Biosystems) under the following conditions: 2 minutes at 50°C, 4 minutes at 95°C, followed by 55 cycles of 15 s at 95°C and 40 s at 55°C Ribosomal 18S RNA or glyceraldehyde-3-phosphate dehydrogenase (GAPDH) mRNA was used as an internal control to normalize the expression levels of each transcript.

cDNA cloning

RNA (5 µg) from bEnd.3 cells was reverse transcribed for 50 minutes at 42°C with Superscript II reverse transcriptase. Partial cDNAs were PCR amplified with Platinum® Pfx DNA polymerase (Invitrogen), with the primers listed in Table S1. The PCR conditions consisted of an initial denaturation step (94°C for 2 minutes), followed by 30 cycles of PCR reaction (94°C for 15 s, 63°C for 30 s, 68°C for 100 s), and then by a final extension step (68°C for 2 minutes). Amplicons were cloned into the PCR-Blunt II-TOPO® vector (Invitrogen) and automatically sequenced from both ends to confirm identity. Before riboprobe synthesis for *in situ* hybridization, the plasmids were linearized with restriction enzymes (Table S1) and purified with the QIAquick® PCR purification kit (Qiagen, Valencia, CA, USA).

Statistical analysis

Unless otherwise stated, means were compared using the unpaired Student's *t*-test or one-way ANOVA when the data met the assumptions of normality (Shapiro–Wilk *W* test) and homogeneity of variance (Levene's test). As an alternative, the Wilcoxon rank-sum or Kruskal–Wallis test was used when the distribution was abnormal or the Welch's *t*-test or Welch's ANOVA when the variances were unequal. The Tukey–Kramer HSD or Dunn's test was used for parametric or nonparametric *post hoc* multiple comparisons, respectively. A two-way ANOVA, followed by the Tukey test, was used when more than one independent variable was being evaluated. Relationships between variables were assessed by Pearson correlation. All these tests used an alpha of 0.05 and were done with JMP® software (SAS Institute, Cary, NC, USA) or Prism® 4 (GraphPad Software, San Diego, CA, USA).

RESULTS

Dexamethasone reduces glioma growth

To assess the effect of dexamethasone on glioma growth, we implanted GL261 glioma cells into the brains of syngeneic immunocompetent mice and treated the animals with either dexamethasone or vehicle. Some mice were killed after 20 days for histological analysis and the remaining mice were monitored for survival. We found that dexamethasone reduced glioma volume by 33% when given twice daily at 1 mg/kg (Figure 1B), but not at a lower dose of 0.1 mg/kg (Student's *t*-test, $P = 0.9$; data not shown). However, glioma-bearing mice treated with the highest dose of dexamethasone did not survive longer than control mice (Figure 1C) and suffered from chronic weight loss (Figure 1D). Therefore, these results indicate that dexamethasone can slow the growth of malignant gliomas, contrary to our expectation, but only at a relatively high concentration and without improving survival, perhaps because of toxic side effects, such as muscle wasting or cachexia (29).

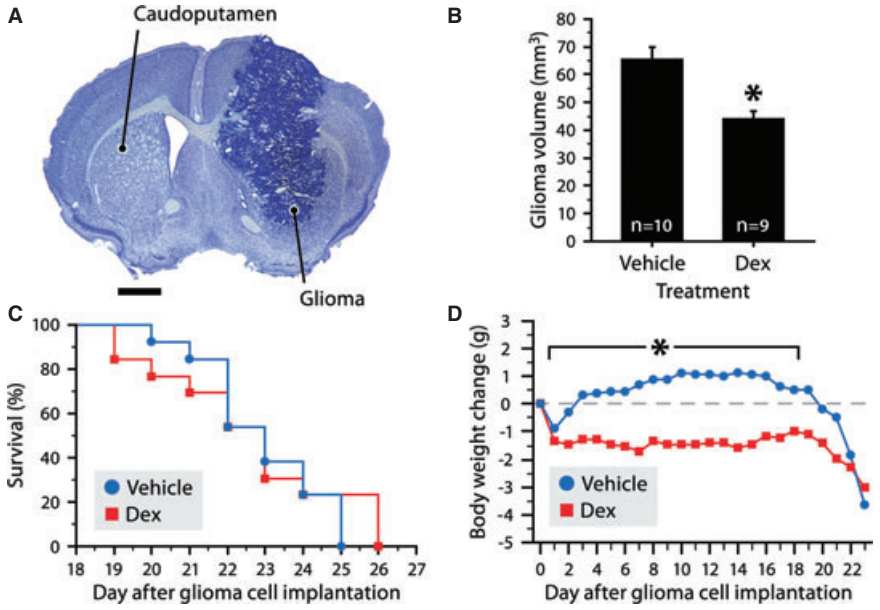

Figure 1. *Dexamethasone reduces the growth of malignant gliomas in mice without increasing survival.* **A.** Representative section of a glioma stained with thionin from a mouse killed 20 days after implantation of GL261 cells into the right caudoputamen. Scale bar, 1 mm. **B.** Stereological analysis revealed a 33% decrease in glioma volume in mice injected twice daily with 1 mg/kg dexamethasone (Dex) compared with sham-treated mice. *Student's *t*-test, $P = 0.0008$. Data show the mean ± SE. **C.** Kaplan–Meier curves showing no difference in the probability of survival between glioma-bearing mice treated or not with dexamethasone (n = 13 per group). Log-rank test, $P = 0.68$. **D.** A chronic reduction in body weight was recorded in glioma-bearing mice treated with dexamethasone (n = 13 per group). *MANOVA with repeated measures ($P < 0.0001$) followed by Student's *t*-tests ($P < 0.02$). The data show mean changes in body weight from the day of tumor implantation.

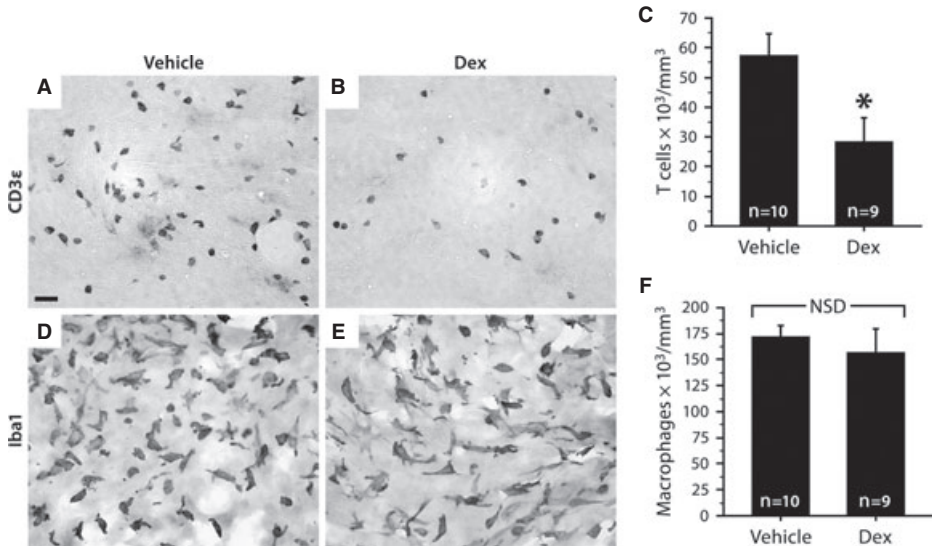

Figure 2. *Dexamethasone depletes tumor-infiltrating T cells, but not macrophages.* **A,B.** T cells immunostained for CD3ε in glioma sections from mice injected twice daily for 20 days with vehicle or 1 mg/kg dexamethasone (Dex), respectively. Scale bar: 20 μm (**A,B,D,E**). **C.** Stereological analysis revealed a 51% decrease in the number of tumor-infiltrating T cells in mice treated with dexamethasone. *Student's *t*-test, $P = 0.017$. Data show the mean ± SE. **D,E.** Macrophages immunostained for Iba1 in glioma sections from mice treated with vehicle or dexamethasone, respectively. Note that macrophage morphology varies among regions (compare **D** with **E**), but that no difference was noted between the treatments. **F.** Stereological analysis showed no intergroup difference in the number of tumor-associated macrophages. Student's *t*-test, $P = 0.5$. Data show the mean ± SE. NSD, not statistically different.

Dexamethasone depletes tumor-infiltrating T lymphocytes

To determine whether dexamethasone had affected, as anticipated, the recruitment of immune cells into the tumors, we immunostained glioma sections for the T cell marker CD3ε (Figure 2A,B) or the macrophage marker Iba1 (Figure 2D,E). Stereological analysis revealed that dexamethasone (1 mg/kg, twice daily) reduced the density of T cells in the tumors by 51% (Figure 2C), but not that of macrophages (Figure 2F). To confirm this decrease and characterize the phenotype of infiltrating T cells, we repeated the experiment, except that tumors were exsanguinated and dissociated into single-cell suspensions for flow cytometric analysis. Multiple labeling with CD3ε, CD4 and CD8 antibodies showed three predominant populations of T cells: $CD4^+$ helper T cells, $CD8^+$ cytotoxic T cells and double-negative ($CD4^-CD8^-$) T cells (Figure 3A–C). In gliomas not exposed to dexamethasone, these populations accounted for 45%, 39% and 15% of the infiltrating T cells, respectively. In agreement with our histological observation, the overall number of infiltrating T cells was 43% lower in dexamethasone-treated mice (Figure 3D). Interestingly, all populations of T cells were equally sensitive to dexamethasone, except double-negative T cells, which were not affected at all (Figure 3E). Further characterization showed that 42% of double-negative T cells expressed the T cell receptor (TCR) ß chain (Figure 3F,I), while another 24% expressed the alternative TCR γδ (Figure 3G,I). Furthermore, 36% of double-negative T cells were positive for the NK cell marker NK-1.1 (Figure 3H,I), which correlated positively with TCR ß (Figure 3J), but negatively with TCR γδ (Figure 3K). Most double-negative T cells were viable, as only 11% on average labeled positively for the apoptotic marker annexin V (data not shown). In summary, our results indicate that dexamethasone can reduce glioma growth while depleting most infiltrating T cells with potential antitumor activity, except a subpopulation including gammadelta and NK T cells.

GL261 cells are resistant to dexamethasone

Although it is unlikely that dexamethasone could be used in human at a dose high enough to inhibit brain tumor growth, we reasoned that understanding the mechanism by which dexamethasone exerts its antitumor effect might help to identify a more specific drug able

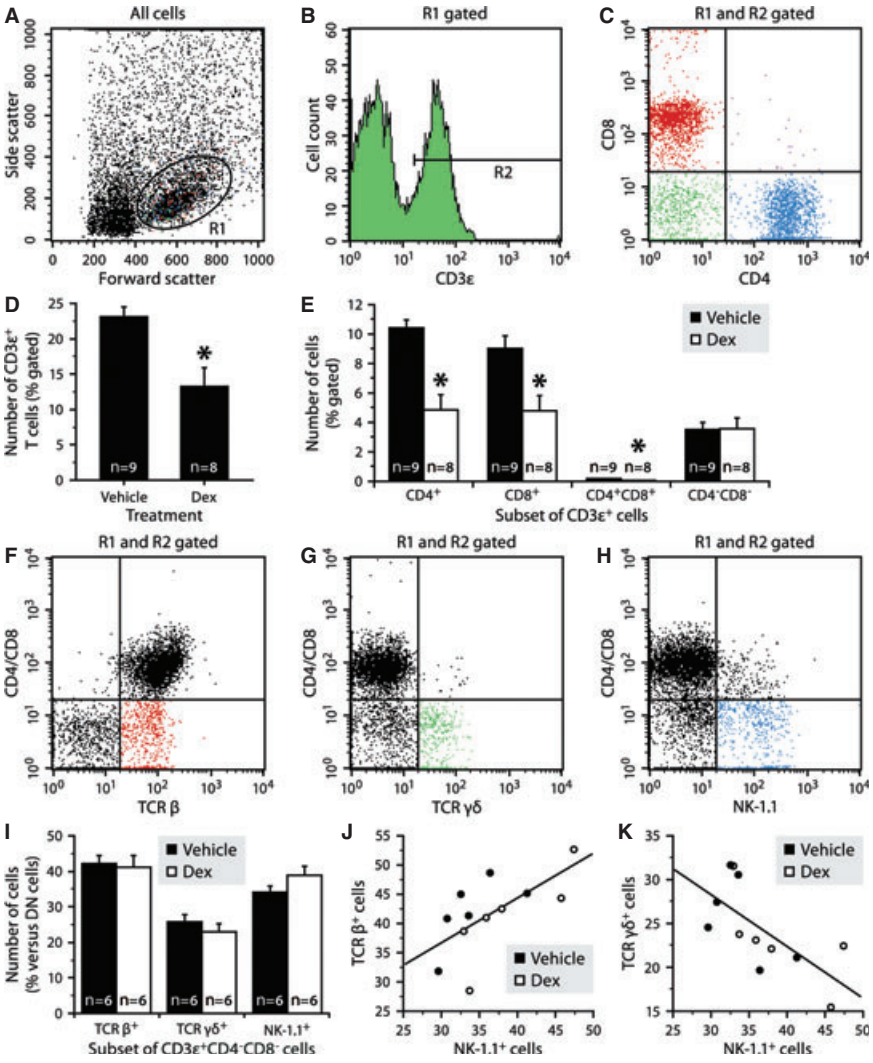

Figure 3. *Dexamethasone selectively depletes tumor-infiltrating T cells with helper or cytotoxic function.* **A–C.** Flow cytometric analysis of cells isolated from a 20-day glioma showing three predominant populations of $CD3\varepsilon^+$ T cells. **D.** Cell counts revealed a 43% decrease in the overall number of $CD3\varepsilon^+$ cells after treatment with dexamethasone (Dex; 1 mg/kg, twice daily). *Welch's *t*-test, $P = 0.0067$. Data show the mean ± SE. **E.** All populations of $CD3\varepsilon^+$ T cells were sensitive to dexamethasone, except $CD4^-CD8^-$ T cells. *Student's *t*-test, $P \leq 0.02$. Data show the mean ± SE. **F–H.** Phenotypic analysis showing $CD3\varepsilon^+CD4^-CD8^-$ T cells positively labeled for T cell receptor (TCR) β (red), TCR γδ (green) and natural killer (NK)-1.1 (blue). **I.** Cell counts showed no change in the number of double negative (DN) T cells expressing TCR β, TCR γδ or NK-1.1 after dexamethasone treatment. Student's *t*-test, $P \geq 0.14$. Data show the mean ± SE. **J,K.** The number of double-negative T cells labeled for NK-1.1 correlated positively with that of TCR β^+ cells (Pearson correlation, $P = 0.022$, $R = 0.65$) and negatively with that of TCR $\gamma\delta^+$ cells (Pearson correlation, $P = 0.016$, $R = -0.68$).

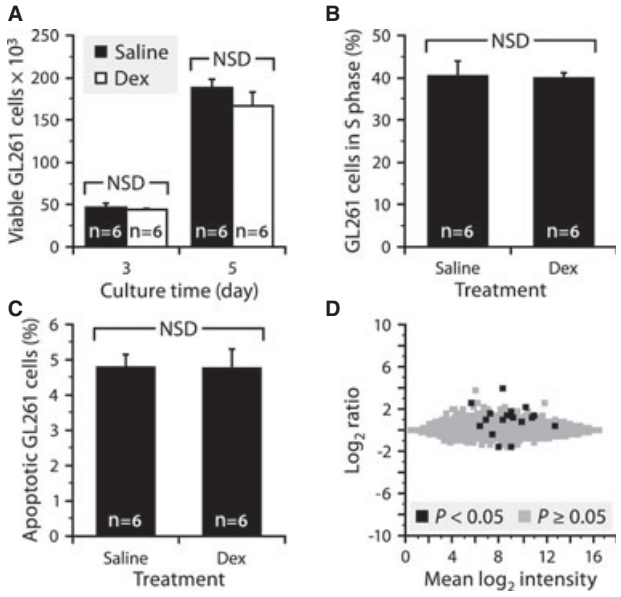

Figure 4. *Cultured GL261 cells are virtually resistant to dexamethasone.* **A.** As determined by flow cytometry, the number of viable cells (propidium iodide negative) did not differ between cultures supplemented or not with 1 μg/mL dexamethasone (Dex). Two-way ANOVA (treatment, $P = 0.23$; time, $P < 0.0001$; interaction, $P = 0.36$). Data show the mean ± SE. NSD, not statistically different. **B.** No difference in the number of cells in the S phase of the cell cycle was detected after a 3-day exposure to dexamethasone (Student's *t*-test, $P = 0.86$). **C.** No difference in the number of apoptotic cells (annexin V positive and propidium iodide negative) was observed between the treatments (Student's *t*-test, $P = 0.31$). **D.** Microarray analysis revealed minor changes in the transcriptional profile of GL261 cells after exposure to dexamethasone for 24 h. Each data point represents one of the 45 101 probe sets. Only 17 of these probe sets (black squares) had a *P*-value <0.05 (see Table S3 for details). *x*-axis, mean of the hybridization intensities of all samples; *y*-axis, ratio of the mean hybridization intensities for dexamethasone-treated cells versus control cells (n = 3 per group).

to mimic dexamethasone's beneficial properties without the side effects. To begin exploring this mechanism, we cultured GL261 cells with or without dexamethasone for 3 or 5 days, and the number of viable cells was then counted by flow cytometry. As shown in Figure 4A, the growth of GL261 cells was not influenced by dexamethasone at a concentration as high as 1 μg/mL. In addition, no intergroup difference in the percentage of cells in the S phase of the cell cycle and the percentage of apoptotic cells was observed (Figure 4B,C), suggesting that dexamethasone does not directly affect the proliferation and survival of GL261 cells. To test whether dexamethasone alters the expression of genes important for tumor progression, we extracted RNA from GL261 cells cultured for 24 h with or without 1 μg/mL dexamethasone. The RNA samples (three per group) were then analyzed using oligonucleotide microarrays interrogating over 39 000 different transcripts. Of those, only 16 genes (represented by 17 probe sets) were identified as being differentially expressed ($P < 0.05$) between treated and control cells (Figure 4D and Table S3), and none had been previously associated with tumor progression, except Enpp2 (also named autotaxin). However, this secreted lysophospholipase, whose expression was upregulated by dexamethasone (Table S3), has recently been shown to promote glioma cell migration *in vitro* (26), which is in contradiction to the possibility that it mediates the antitumor effect of dexamethasone. Overall, these results indicate that GL261 cells are largely insensitive to dexamethasone, suggesting that this drug reduces glioma growth by an indirect mechanism.

Dexamethasone decreases glioma vascularization

It has been shown that glioma cells, including GL261 cells, grow by co-opting pre-existing blood vessels, which undergo morphological and functional changes and even regress to some extent (12, 15, 19, 50). As shown in Figure 5A–C, the capillaries of GL261 gliomas are hypertrophied and irregularly shaped compared with those of the adjacent normal tissue. Because these changes are presumably important for glioma growth, we asked whether dexamethasone could normalize certain vascular parameters, such as capillary density and caliber. To address this question, glioma sections, from mice treated or not with dexamethasone and killed 20 days after tumor implantation, were immunostained for the endothelial marker CD31 and analyzed using unbiased stereological methods. We found a slightly decreased tumor vascular density in dexamethasone-treated mice (Figure 5D), but no significant difference in tumor vessel diameter (Figure 5E), although a tendency to decrease was observed. However, the volume of the tumors correlated better with vessel diameter (Figure 5F) than with vascular density (Figure 5G). Therefore, these results suggest that although dexamethasone acts on the tumor endothelium, its antineoplastic effect is not a consequence of the reduction in vascularization.

Dexamethasone reduces Angpt2 expression

An alternative hypothesis is that dexamethasone modulates the production of proneoplastic or antineoplastic factors by tumor endothelial cells. To investigate this possibility in a simplified model, we used oligonucleotide microarrays to compare the gene expression profiles of cerebral endothelial cells cultured for 24 h with or without dexamethasone (1 μg/mL; n = 3 per group). In contrast to what we observed with GL261 cells (Table S3), 1253 dexamethasone-sensitive genes (represented by 1455 probe sets) with a *P*-value <0.05 were found (Figure 6A and Table S4). To narrow our search, we arbitrarily chose to filter out probe sets with a fold change between 0.5 and 2.0, and retained only those classified as "extracellular" in the Gene Ontology database, because of their potential therapeutic value. Among the 83 remaining genes, we selected for further analysis four down-regulated ones, namely Angpt2, Tnc and TGFß2, which are known to be associated with certain cancers (5, 11, 34), and ESM1, a newly discovered proteoglycan that has been shown to induce tumor formation (36). Quantitative RT-PCR analysis confirmed that all these genes were strongly repressed by dexamethasone at all doses tested in cultured cerebral endothelial cells (Figure 6B–E). These results were not caused by nonspecific toxicity, because the upregulation of genes observed by microarray was confirmed by quantitative RT-PCR (e.g. in Figure 6F).

To validate these results in a more complex, *in vivo* system, glioma-bearing mice were injected twice daily with 1 mg/kg dex-

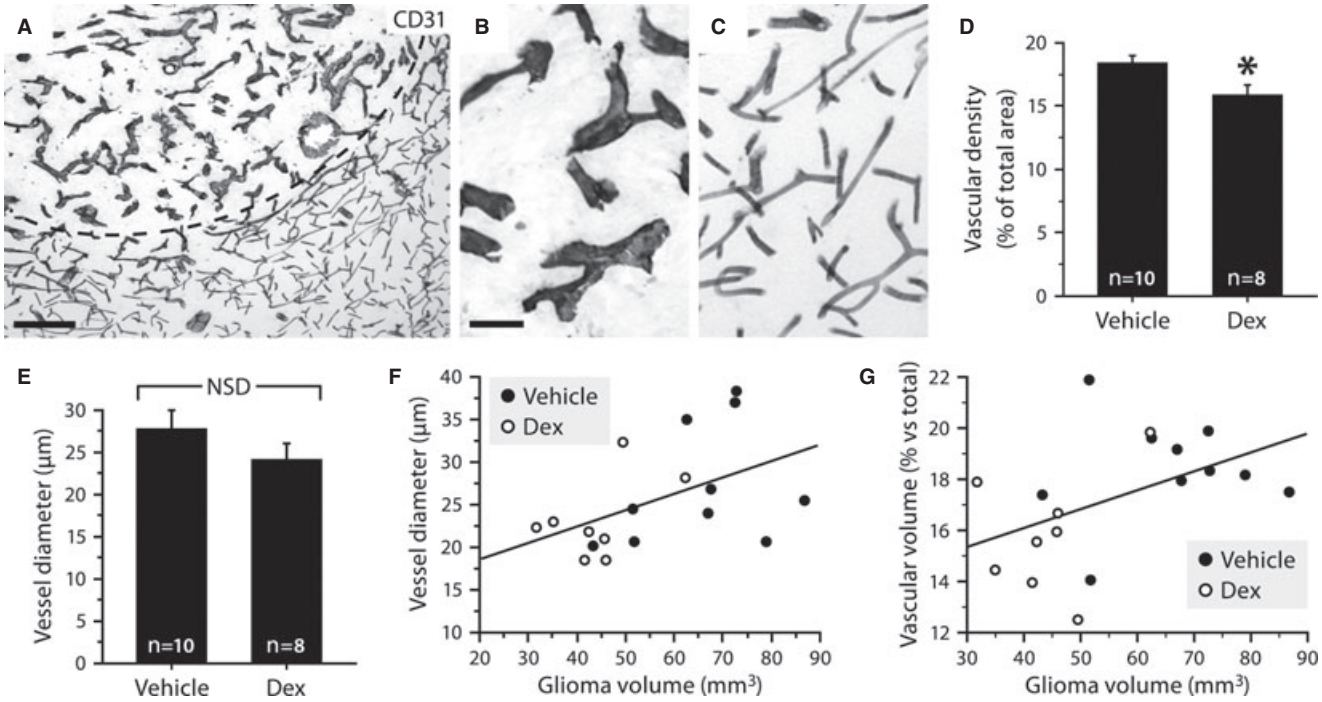

Figure 5. *Dexamethasone slightly reduces tumor vascular density.* **A.** Glioma section immunostained for CD31 showing morphological differences between the tumor and adjacent normal vasculature. The dashed line separates the tumor (top) from the nonneoplastic tissue (bottom). Scale bar: 200 µm. **B,C.** Higher magnification of capillaries in a glioma and the adjacent nonneoplastic tissue, respectively. Scale bar: 50 µm (**B,C**). **D.** Stereological analysis revealed a 14% decrease in tumor vascular density in mice treated twice daily with 1 mg/kg dexamethasone compared with mock-treated mice. *Student's *t*-test, $P = 0.024$. Data show the mean ± SE. **E.** No difference in tumor vessel caliber was recorded between mice treated or not with dexamethasone. Wilcoxon rank-sum test, $P = 0.2$. Data show the mean ± SE. **F,G.** Glioma volume correlated better with vessel diameter (**F**, Pearson correlation, $P = 0.041$, $R = 0.49$) than with vascular volume (**G**, Pearson correlation, $P = 0.053$, $R = 0.46$). Each data point represents a mouse treated with dexamethasone or vehicle.

amethasone for 2 or 3 weeks, and their brains were collected for *in situ* hybridization analysis. Two of the examined transcripts (TGFß2 and ESM1) were not reliably detected and were thus excluded from the study at this point (data not shown). Conversely, strong hybridization signals for Angpt2 and Tnc mRNAs were specifically detected along the tumor vasculature and not in the surrounding nonneoplastic tissue (Figure 7A,B,E). Stereological analysis revealed an approximately 40% decrease in the number of Angpt2 mRNA$^+$ cells within the tumors of dexamethasone-treated mice at both time points (Figure 7C), but no change in Tnc mRNA$^+$ cells (Figure 7F). To support this result, we estimated the intensity of the hybridization signals for Angpt2 mRNA at the single-cell level by optical density readings and found that the signals in dexamethasone-treated mice were 38 and 27% less intense than those in controls at 2 and 3 weeks, respectively (Figure 7D). In other words, not only were there fewer Angpt2 mRNA$^+$ cells in dexamethasone-treated mice, but these positive cells also expressed lower levels of Angpt2 mRNA. These results suggest that dexamethasone could influence glioma vascularization and growth, at least in part, by inhibiting the expression of Angpt2, which is known to be a destabilizing factor for the endothelium (34).

It has been reported that Angpt2 can induce glioma cell invasion by stimulating MMP2 expression (20, 21), which could thus be indirectly repressed by dexamethasone. Furthermore, it has been suggested that dexamethasone can reduce brain tumor-associated vascular permeability by inhibiting VEGFa expression (18, 28). To determine whether these two genes are repressed in the model used here, we quantified MMP2 and VEGFa mRNAs in our RNA and tissue samples by qRT-PCR and *in situ* hybridization, respectively. We found that MMP2 was down-regulated by dexamethasone in cultured cerebral endothelial cells, but not in gliomas of mice treated for 2 or 3 weeks with the steroid, whereas VEGFa was not affected by dexamethasone, neither *in vitro* nor *in vivo* (Figure 8).

Selective inhibition of Angpt2 reduces glioma growth

Although Angpt2 is known to be expressed in human and experimental gliomas (43), its importance in the growth of these tumors is still unclear. To test the possibility that pharmacological neutralization of Angpt2 reproduces the effects of dexamethasone on glioma growth and vascularization, we treated glioma-bearing mice every other day with an anti-Angpt2 peptide-Fc fusion protein called L1-10, which has recently been used with success to inhibit the development of epidermoid and colorectal tumor xenografts (30). Remarkably, we found that L1-10 reduced glioma volume by 50% (Figure 9A), as evaluated in mice killed 18 days after tumor implantation. Although L1-10 did not cure glioma-bearing mice, it produced a modest increase in their survival (Figure 9B). No

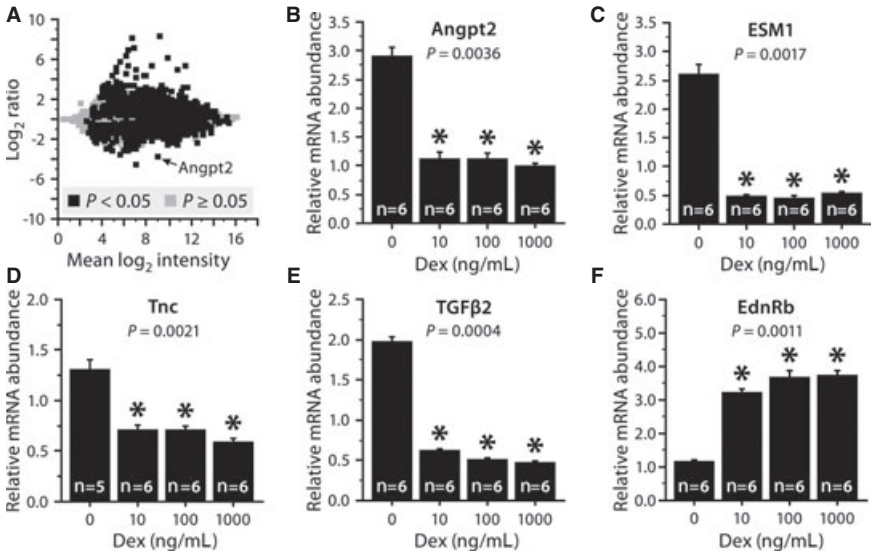

Figure 6. *Genes modulated by dexamethasone in cultured cerebral endothelial cells*. **A.** Microarray analysis revealed major changes in the transcriptional profile of bEnd.3 cells after exposure to dexamethasone for 24 h. Each data point represents one of the 45 101 probe sets; 1455 of these probe sets (black squares) had a *P*-value <0.05 (see Table S4 for details). *x*-axis, mean of the hybridization intensities of all samples; *y*-axis, ratio of the mean hybridization intensities for dexamethasone-treated cells versus control cells (n = 3 per group). **B–F.** Quantitative RT-PCR analysis confirmed the differential expression of Angpt2, ESM1, Tnc, TGFβ2 and EdnRb mRNAs in bEnd.3 cells cultured for 24 h in the presence of different concentrations of dexamethasone (Dex) compared with mock-treated cells. *Kruskal–Wallis test (*P* as indicated) followed by Dunn's test. The data (mean ± SE) are expressed as a ratio to 18S rRNA. Repeat analysis of Angpt2 with normalization to GAPDH mRNA instead of 18S rRNA gave similar results (data not shown).

noticeable side effect, such as chronic reduction in body weight, was associated with the use of L1-10 (Figure 9C). The antitumor effect of L1-10 was indirect, because the growth of GL261 cells *in vitro* was not altered after addition of 5 μM L1-10 to the culture media (Figure 9D). To examine the effect of L1-10 on tumor vasculature, we immunostained glioma sections for CD31 and found a small (9%) but significant decrease in tumor vascular density in L1-10-treated mice (Figure 9E), as observed in the case of dexamethasone (Figure 5D). In contrast to dexamethasone, L1-10 reduced tumor vessel diameter by 29% (Figure 9F), which strongly correlated with glioma volume (Figure 9G). Finally, because it has recently been shown that Angpt2 is involved in inflammatory processes (14), we tested whether L1-10 influenced the recruitment of immune cells into the tumors. Stereological analysis of sections immunostained for CD3e or Iba1 revealed no significant difference in T cells (Figure 9H), but a small reduction (17%) in macrophages (Figure 9I). Collectively, our results ascribed to Angpt2 an important role in glioma development and support the concept that dexamethasone slows glioma growth by a mechanism involving the attenuation of Angpt2 expression.

DISCUSSION

Dexamethasone is one of the most commonly prescribed drugs and has been used since the 1960s for the management of edema associated with brain tumors; however, its effects on these tumors are not fully understood. The initial hypothesis tested in this work was that dexamethasone accelerates glioma growth by antagonizing antitumor immune responses. Although this hypothesis proved to be incorrect, four main findings emerged from our work: (i) dexamethasone can exert potential proneoplastic effects by neutralizing important components of the immune system (i.e. cytotoxic and helper T cells); (ii) dexamethasone can also exert antineoplastic effects by reducing the expression of at least one angiogenic factor, Angpt2, leading to a partial normalization of the tumor vasculature; (iii) the sum of the actions of dexamethasone results in a reduction of glioma growth, but only when it is used at a relatively high concentration associated with adverse effects; and (iv) selective blocking of Angpt2 with a peptide-Fc fusion protein reduces glioma growth and vascular enlargement more efficiently than dexamethasone without depleting tumor-infiltrating T lymphocytes or causing notable side effects. This greater efficiency of L1-10 is presumably caused by a more complete neutralization of Angpt2, because dexamethasone only partially inhibits its expression.

Although the matrix-degrading enzyme MMP2 and the angiogenic regulator VEGFa were expressed in our glioma model and might play important growth-promoting roles, our results do not support their involvement in the mechanism by which dexamethasone reduced glioma growth. On one hand, we expected that dexamethasone would reduce MMP2 expression *in vivo*, at least indirectly, because it has been reported that Angpt2 stimulates glioma cells to produce MMP2 (20, 21), and because we found a reduction in MMP2 mRNA in cultured endothelial cells exposed to dexamethasone. However, no change in MMP2 expression was detectable *in vivo* after dexamethasone treatment. This lack of effect may be caused by a difference between the glioma cells studied: GL261 cells strongly and constitutively

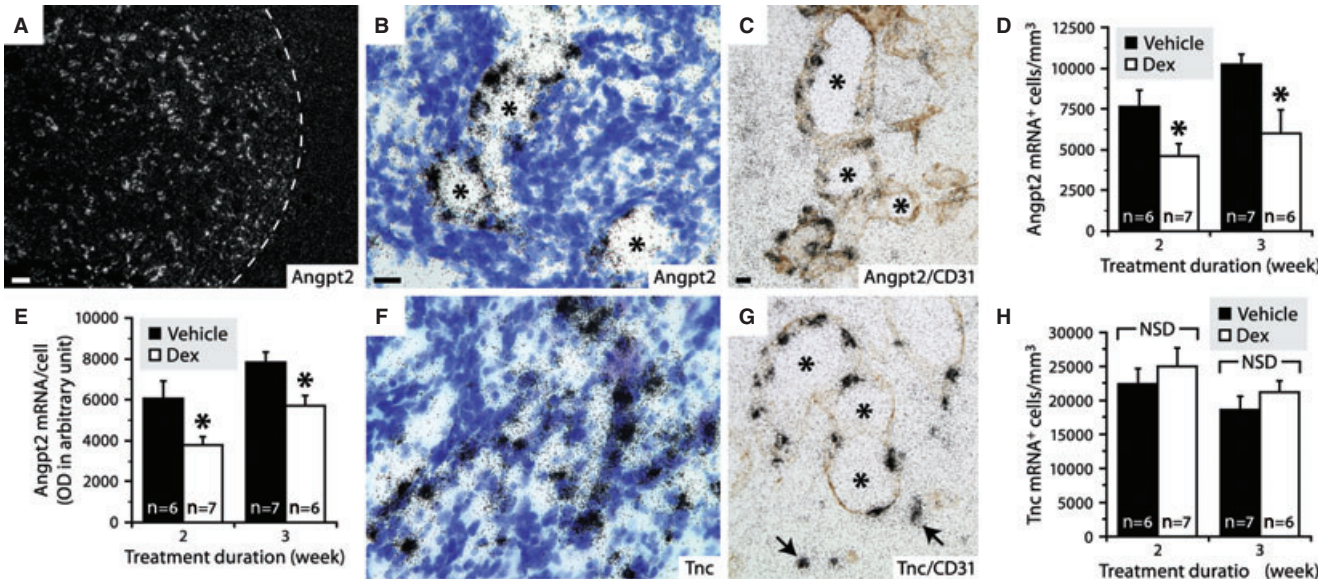

Figure 7. *Dexamethasone inhibits the endothelial expression of Angpt2 in gliomas, but not that of Tnc.* **A.** Dark-field photomicrograph showing *in situ* hybridization signals for Angpt2 mRNA in a 20-day glioma. The dashed line separates the tumor (left) from the normal tissue (right). Scale bar: 500 μm. **B.** Bright-field image at higher magnification of *in situ* hybridization signals for Angpt2 mRNA (black grains). Blue, thionin counterstaining. *Blood vessel. Scale bar: 20 μm (**B,E**). **C.** Double labeling for Angpt2 mRNA (*in situ* hybridization, black grains) and CD31 (immunohistochemistry, brown). *Blood vessel lumen. Scale bar: 20 μm (**C,G**). **D.** Stereological analysis revealed that the number of Angpt2 mRNA$^+$ cells was approximately 40% lower in mice treated for 2 or 3 weeks with 1 mg/kg dexamethasone compared with sham-treated mice. *Two-way ANOVA (treatment, $P = 0.0019$; time, $P = 0.065$; interaction, $P = 0.56$) followed by Student's *t*-test. Data show the mean ± SE. **E.** Optical density (OD) analysis of hybridization signals showed that the abundance of Angpt2 mRNA per positive cell was reduced by 38% at 2 weeks after dexamethasone treatment and by 27% at 3 weeks after dexamethasone treatment. *Two-way ANOVA (treatment, $P = 0.0016$; time, $P = 0.0058$; interaction, $P = 0.87$) followed by Student's *t*-test. Data show the mean ± SE. **F.** Bright-field image of *in situ* hybridization signals for Tnc mRNA (black grains). Blue, thionin counterstaining. **G.** Double labeling for Tnc mRNA (*in situ* hybridization, black grains) and CD31 (immunohistochemistry, brown). Note that Tnc mRNA did not always colocalize with CD31 (arrows). *Blood vessel lumen. **H.** No intergroup difference in the number of Tnc mRNA$^+$ cells was detected. Two-way ANOVA (treatment, $P = 0.42$; time, $P = 0.12$; interaction, $P = 0.99$). Data show the mean ± SE. NSD, not statistically different.

expressed MMP2 after transplantation, whereas the human cell lines used by Hu and colleagues expressed MMP2 in an inducible-manner at the invasive border of the tumor (20). Therefore, we cannot exclude the possibility that dexamethasone can reduce the progression of other types of glioma cells by inhibiting MMP2 when this factor is not constitutively produced. On the other hand, we also expected a down-regulation of VEGFa expression by dexamethasone on the basis of two *in vitro* studies (18, 28). Although the different nature of the cells used may again explain the difference in our results, it is important to note that one of the research teams did not attempt to confirm their results *in vivo* (18), while the other group did not reproduce the same effect in a subcutaneous glioma model (28). Similar to the latter study, we found genes (MMP2 and Tnc) that were sensitive to dexamethasone in culture, but not *in vivo*, possibly because of differences in pharmacokinetic or the regulatory mechanisms involved. Together, these observations underscore the necessity of confirming *in vitro* results in more clinically relevant *in vivo* models.

It has been reported that anti-Angpt2 antibodies can inhibit the growth of subcutaneously implanted tumors and induce their regression (30). In contrast, our results indicate that gliomas can only be slowed and not cured by anti-Angpt2 therapy. This difference may be explained by several possibilities. First, orthotopic gliomas are probably less dependent on angiogenesis than heterotopic tumors developing in the subcutaneous space. Indeed, it has been shown that GL261 cells and other glioma cells mainly grow by co-opting existing capillaries and that new blood vessels are only formed in a late phase in response to hypoxia or cell death (12, 15, 19, 50). Second, the bioavailability of L1-10 might be lower in gliomas compared with peripheral tumors because of the presence of the blood–brain barrier. In future studies, it will be important to examine whether the effectiveness of L1-10 against cerebral tumors can be enhanced by using a higher dose or an alternative delivery method. Third, it is possible that GL261 cells are more resistant to hypoxia or inadequate supply of serum growth factors than other tumor cell lines. It remains to be determined whether all types of glioma cells are equally sensitive to Angpt2 inhibitors, ideally in a clinical setting, or alternatively, using syngeneic and orthotopic models. Finally, we cannot exclude the possibility that another angiogenic factor partially compensates for the reduction in Angpt2 in gliomas, although no naturally occurring agonist of Angpt2 is currently known, except perhaps Angpt3 (46). However, the latter was not detectable in GL261 gliomas by *in situ* hybridization (unpublished personal observation).

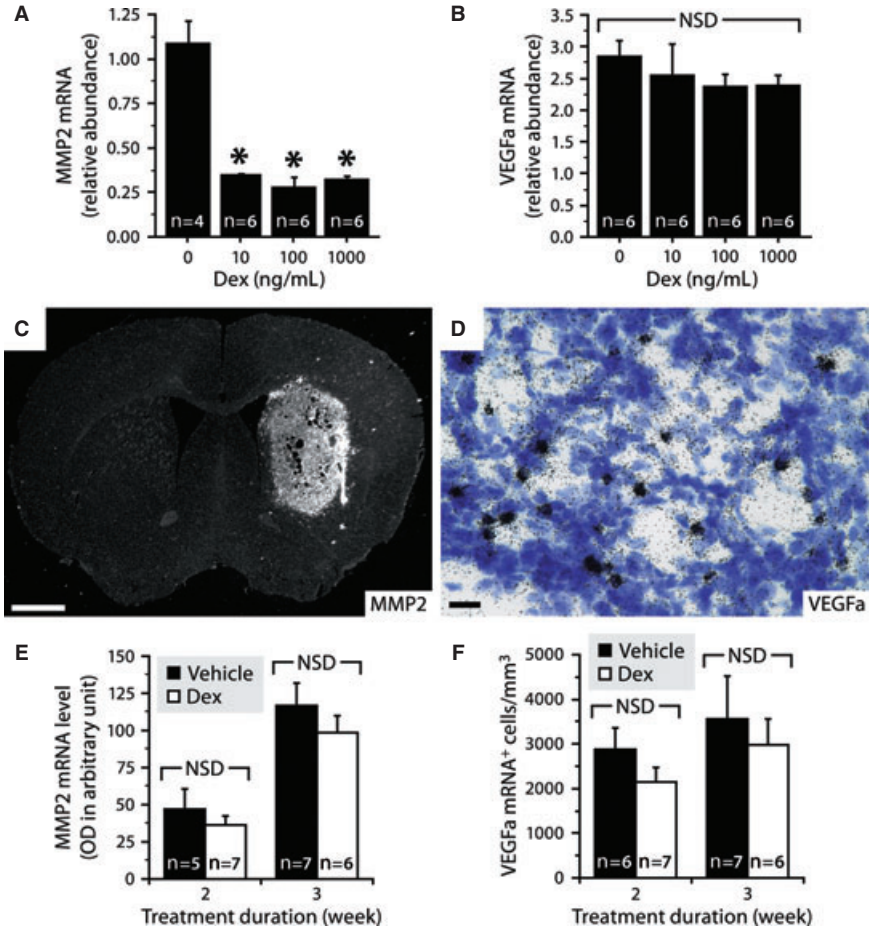

Figure 8. *Dexamethasone does not affect MMP2 and VEGFa expression* in vivo, *but reduces MMP2 expression* in vitro. **A,B.** Quantitative RT-PCR analysis showed reduced levels of MMP2 mRNA, but not of VEGFa mRNA, in bEnd.3 cells cultured for 24 h in the presence of different concentrations of dexamethasone (Dex) compared with mock-treated cells. *Kruskal–Wallis test ($P = 0.0173$) followed by Dunn's test. Data (mean ± SE) are expressed as a ratio to 18S rRNA. **C.** Dark-field photomicrograph of *in situ* hybridization signals for MMP2 mRNA in a 2-week glioma. Note that MMP2 expression is not restricted to the endothelium, but is widespread in the tumor. Scale bar: 1 mm. **D.** Bright-field photomicrograph of *in situ* hybridization signals for VEGFa mRNA (black grains) in a 3-week glioma. Blue, thionin counterstaining. Scale bar: 20 µm. **E.** Optical densitometric analysis revealed no difference in MMP2 mRNA levels in mice treated or not with 1 mg/kg dexamethasone. *Two-way ANOVA (treatment, $P = 0.24$; time, $P < 0.0001$; interaction, $P = 0.79$). Data show the mean ± SE. **F.** Stereological analysis revealed no difference in the number of VEGFa mRNA$^+$ cells in mice treated or not with 1 mg/kg dexamethasone. *Two-way ANOVA (treatment, $P = 0.25$; time, $P = 0.06$; interaction, $P = 0.12$). Data show the mean ± SE.

During glioma progression, the vasculature undergoes structural and functional changes, resulting in vascular cell apoptosis and blood vessel regression. It has been postulated that this regression is caused by the action of Angpt2 in the absence of VEGFa (15, 19, 50). Our results do not support this concept because VEGFa was expressed at all time points examined, and L1-10 treatment reduced vascular density, suggesting rather that Angpt2 somehow limits vascular regression in our model. However, this effect does not explain the proneoplastic activity of Angpt2 because we observed no clear correlation between vascular density and glioma volume. Another effect of Angpt2 that did correlate with glioma volume is the increase in vascular caliber. We propose that this effect is accompanied by changes in vascular physiology and that some of those are directly responsible for the proneoplastic activity of Angpt2. At least four scenarios can be imagined: (i) Angpt2 could increase vascular permeability, thereby providing glioma cells with better access to nutrients and growth factors; (ii) it could induce edema that could contribute to destruction of peritumor tissue and thus facilitate glioma cell invasion; (iii) it could induce structural alterations in the vascular wall that would facilitate the process of co-option and the migration of glioma cells along the vasculature, a phenomenon recently observed (12); and (iv) it could promote the recruitment of a subpopulation of monocytic cells with pro-angiogenic activity, identified as Tie2-expressing monocytes (8), by stimulating the expression of adhesion molecules, such as ICAM1 and VCAM1 (14). This latter effect would explain the reduction in tumor-associated macrophages observed after L1-10 treatment.

It is generally known that glucocorticoids can deplete lymphocytes by inducing apoptosis and inhibiting the expression of adhesion molecules and cytokines involved in their recruitment across the endothelium (1). The reduced number of tumor-infiltrating helper and cytotoxic T cells observed after dexamethasone treatment in this study was thus predictable. However, we did not expect the discovery of a new property of gammadelta and NK T cells, that of being resistant to dexamethasone. Gammadelta T cells are different from other T lymphocytes in their ability to recognize soluble protein and nonprotein antigens in a major histocompatibility complex (MHC)-independent manner (4). NK T cells are also MHC-unrestricted, but mainly recognize glycolipids presented by the CD1d molecule (27). Mounting evidence suggests that most gammadelta and NK T cells contribute to antitumor immunity by exerting cytotoxic effects or influencing the activity of other cell types by secreting a variety of cytokines (13, 24, 37). On the contrary, a subset of NK T cells known as Type II has been shown to repress antitumor immune responses (37, 44). Interestingly, we found an inverse correlation between gammadelta and NK T cells, but further investigation is required to determine the significance of this observation; for example, it will be interesting to test whether one cell type inhibits the other. Nevertheless, it could be useful to develop immunotherapy using gammadelta and NK T cells, not

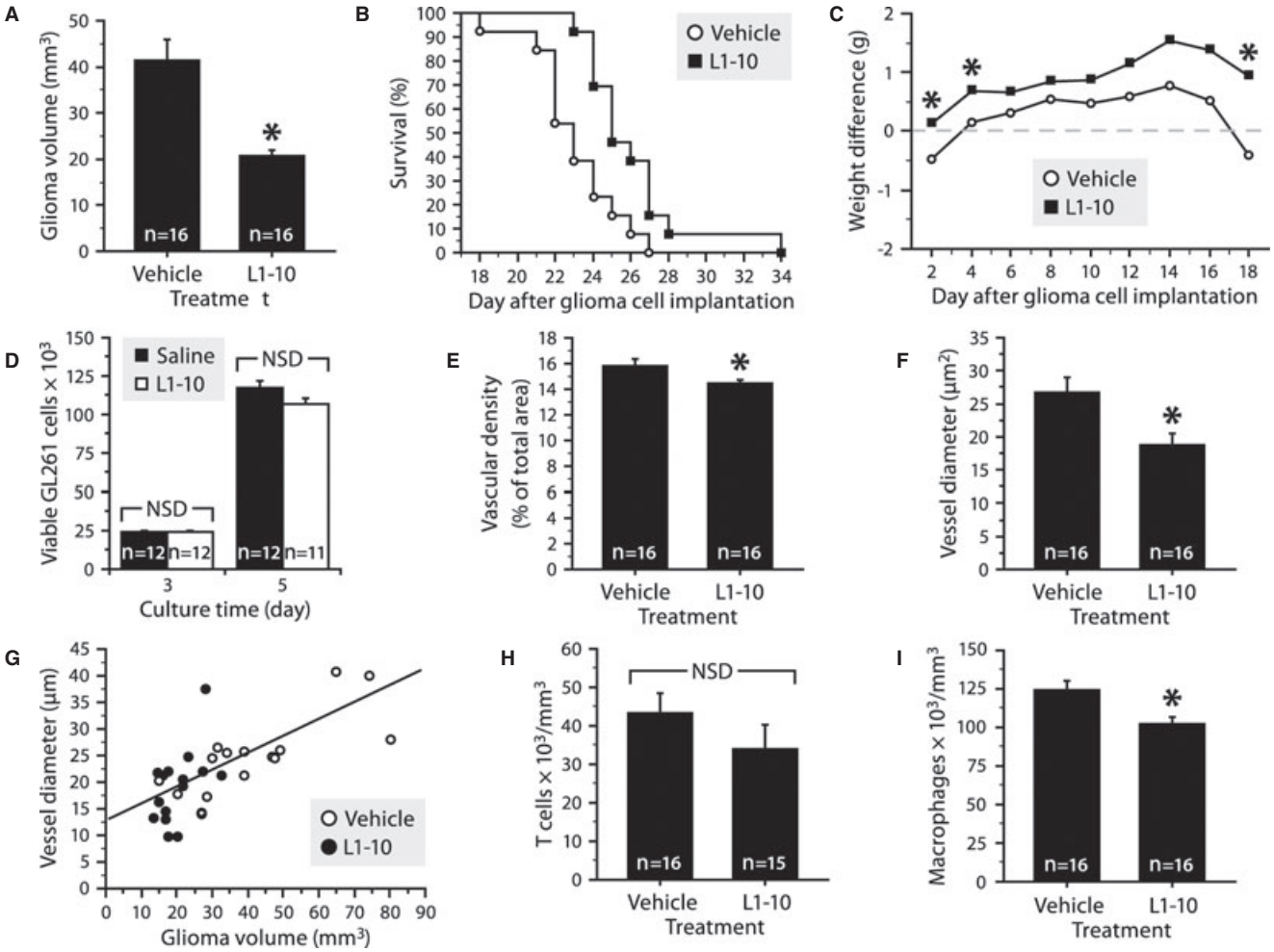

Figure 9. *Specific neutralization of Angpt2 with L1-10 reduces glioma growth and vascular enlargement without affecting T cell infiltration.* **A.** Volumetric analysis showed a 50% decrease in glioma volume in L1-10-treated mice. *Wilcoxon rank-sum test, $P = 0.0002$. Data show the mean ± SE. **B.** Increases in body weight were recorded at the beginning and at the end of experimentation in mice injected with L1-10. *MANOVA with repeated measures ($P = 0.002$) followed by Student's *t*-test ($P < 0.05$). The data show the mean change in body weight from the day of tumor implantation (n = 16 per group). **C.** Kaplan–Meier curves showing a modest increase in the probability of survival after treatment with dexamethasone. Log-rank test, $P = 0.005$ (n = 13 per group). **D.** As determined by flow cytometry, the growth of GL261 cells in culture was not affected in the presence of 5 µM L1-10. Two-way ANOVA (treatment, $P = 0.1$; time, $P < 0.0001$; interaction, $P = 0.07$). Data show the mean ± SE. NSD, not statistically different. **E.** Stereological analysis revealed a 9% decrease in tumor vascular density in L1-10-treated mice. *Wilcoxon rank-sum test, $P = 0.03$. Data show the mean ± SE. **F,G.** Tumor vessel diameter was reduced by 29% in L1-10-treated mice and correlated positively with glioma volume (Pearson correlation, $P = 0.0002$, $R = 0.61$). *Wilcoxon rank-sum test, $P = 0.0053$. Each data point represents a mouse treated with L1-10 or vehicle. **H.** No intergroup difference was detected in $CD3^+$ T cell density. Wilcoxon rank-sum test, $P = 0.07$. Data show the mean ± SE. **I.** A 17% decrease in the number of tumor-associated $Iba1^+$ macrophages was observed after L1-10 treatment. Wilcoxon rank-sum test, $P = 0.004$. Data show the mean ± SE.

only because patients with brain tumors are treated with dexamethasone, but also because MHC alleles are frequently downregulated during cancer progression. Our ability to manipulate these cells for therapeutic purposes will depend on a better understanding of their roles and the mechanisms that govern their development and activities. In the meantime, the finding that NK T cells collected from patients with glioma can kill glioma cells in culture is encouraging (9).

In conclusion, this study not only helps to better understand the effects of dexamethasone on brain tumors, but also reveals a more specific agent, L1-10, that mimics beneficial properties of dexamethasone without the detrimental effects. In future work, it will be necessary to determine whether the effects of dexamethasone and the efficiency of L1-10 are similar for most gliomas or if they vary depending on the nature of the tumor. It will also be important to evaluate whether Angpt2 inhibitors could replace dexamethasone or be used in combination with it, and whether they could enhance the efficacy of chemotherapeutic drugs, as recently proposed (25). Finally, it will be interesting to compare the effects of dexamethasone in mice deficient or not in Angpt2 to verify whether its antitu-

mor action results only from the inhibition of Angpt2 or whether other proneoplastic factors are affected. The identification of such factors would provide additional potential targets for the treatment of malignant cerebral tumors.

ACKNOWLEDGMENTS

This work was supported by the Cancer Research Society, the Canadian Institutes for Health Research (CIHR) and the Canada Foundation for Innovation. L.V. received a Career Award from the Rx&D Health Research Foundation and CIHR. J.V. was supported by studentships from the CIHR and the *Fonds de la Recherche en Santé du Québec*. M.J.B. was supported by the Laurye Lapointe Foundation. A.C. is a member of the *Carrera del Investigador, Consejo de Investigaciones Científicas y Técnicas*, Argentina. We thank Maurice Dufour, Ezequiel Calvo and the Gene Quantification Core Laboratory of the Quebec Genomics Center for assistance with flow cytometry, microarray analysis, and quantitative PCR, respectively.

REFERENCES

1. Ashwell JD, Lu FW, Vacchio MS (2000) Glucocorticoids in t cell development and function. *Annu Rev Immunol* **18**:309–345.
2. Benedetti S, Pirola B, Poliani PL, Cajola L, Pollo B, Bagnati R *et al* (2003) Dexamethasone inhibits the anti-tumor effect of interleukin 4 on rat experimental gliomas. *Gene Ther* **10**:188–192.
3. Brooks WH, Markesbery WR, Gupta GD, Roszman TL (1978) Relationship of lymphocyte invasion and survival of brain tumor patients. *Ann Neurol* **4**:219–224.
4. Carding SR, Egan PJ (2002) Gammadelta T cells: functional plasticity and heterogeneity. *Nat Rev Immunol* **2**:336–345.
5. Chiquet-Ehrismann R, Chiquet M (2003) Tenascins: regulation and putative functions during pathological stress. *J Pathol* **200**:488–499.
6. Das A, Banik NL, Patel SJ, Ray SK (2004) Dexamethasone protected human glioblastoma U87MG cells from temozolomide induced apoptosis by maintaining Bax:bcl-2 ratio and preventing proteolytic activities. *Mol Cancer* **3**:36.
7. De Bosscher K, Vanden Berghe W, Haegeman G (2003) The interplay between the glucocorticoid receptor and nuclear factor-kappaB or activator protein-1: molecular mechanisms for gene repression. *Endocr Rev* **24**:488–522.
8. De Palma M, Venneri MA, Galli R, Sergi Sergi L, Politi LS, Sampaolesi M, Naldini L (2005) Tie2 identifies a hematopoietic lineage of proangiogenic monocytes required for tumor vessel formation and a mesenchymal population of pericyte progenitors. *Cancer Cells* **8**:211–226.
9. Dhodapkar KM, Cirignano B, Chamian F, Zagzag D, Miller DC, Finlay JL, Steinman RM (2004) Invariant natural killer T cells are preserved in patients with glioma and exhibit antitumor lytic activity following dendritic cell-mediated expansion. *Int J Cancer* **109**:893–899.
10. Ehtesham M, Black KL, Yu JS (2004) Recent progress in immunotherapy for malignant glioma: treatment strategies and results from clinical trials. *Cancer Control* **11**:192–207.
11. Elliott RL, Blobe GC (2005) Role of transforming growth factor Beta in human cancer. *J Clin Oncol* **23**:2078–2093.
12. Farin A, Suzuki SO, Weiker M, Goldman JE, Bruce JN, Canoll P (2006) Transplanted glioma cells migrate and proliferate on host brain vasculature: a dynamic analysis. *Glia* **53**:799–808.
13. Ferrarini M, Ferrero E, Dagna L, Poggi A, Zocchi MR (2002) Human gammadelta T cells: a nonredundant system in the immune-surveillance against cancer. *Trends Immunol* **23**:14–18.
14. Fiedler U, Reiss Y, Scharpfenecker M, Grunow V, Koidl S, Thurston G *et al* (2006) Angiopoietin-2 sensitizes endothelial cells to TNF-alpha and has a crucial role in the induction of inflammation. *Nat Med* **12**:235–239.
15. Fischer I, Gagner JP, Law M, Newcomb EW, Zagzag D (2005) Angiogenesis in gliomas: biology and molecular pathophysiology. *Brain Pathol* **15**:297–310.
16. Gagner JP, Law M, Fischer I, Newcomb EW, Zagzag D (2005) Angiogenesis in gliomas: imaging and experimental therapeutics. *Brain Pathol* **15**:342–363.
17. Galarneau H, Villeneuve J, Gowing G, Julien JP, Vallières L (2007) Increased glioma growth in mice depleted of macrophages. *Cancer Res* **67**:8874–8881.
18. Heiss JD, Papavassiliou E, Merrill MJ, Nieman L, Knightly JJ, Walbridge S *et al* (1996) Mechanism of dexamethasone suppression of brain tumor-associated vascular permeability in rats. Involvement of the glucocorticoid receptor and vascular permeability factor. *J Clin Invest* **98**:1400–1408.
19. Holash J, Maisonpierre PC, Compton D, Boland P, Alexander CR, Zagzag D *et al* (1999) Vessel cooption, regression, and growth in tumors mediated by angiopoietins and VEGF. *Science* **284**:1994–1998.
20. Hu B, Guo P, Fang Q, Tao HQ, Wang D, Nagane M *et al* (2003) Angiopoietin-2 induces human glioma invasion through the activation of matrix metalloprotease-2. *Proc Natl Acad Sci USA* **100**:8904–8909.
21. Hu B, Jarzynka MJ, Guo P, Imanishi Y, Schlaepfer DD, Cheng SY (2006) Angiopoietin 2 induces glioma cell invasion by stimulating matrix metalloprotease 2 expression through the alphavbeta1 integrin and focal adhesion kinase signaling pathway. *Cancer Res* **66**:775–783.
22. Jemal A, Siegel R, Ward E, Murray T, Xu J, Thun MJ (2007) Cancer statistics, 2007. *CA Cancer J Clin* **57**:43–66.
23. Kaal EC, Vecht CJ (2004) The management of brain edema in brain tumors. *Curr Opin Oncol* **16**:593–600.
24. Kabelitz D, Wesch D, Pitters E, Zoller M (2004) Potential of human gammadelta T lymphocytes for immunotherapy of cancer. *Int J Cancer* **112**:727–732.
25. Kerbel RS (2006) Antiangiogenic therapy: a universal chemosensitization strategy for cancer? *Science* **312**:1171–1175.
26. Kishi Y, Okudaira S, Tanaka M, Hama K, Shida D, Kitayama J *et al* (2006) Autotaxin is overexpressed in glioblastoma multiforme and contributes to cell motility of glioblastoma by converting lysophosphatidylcholine to lysophosphatidic Acid. *J Biol Chem* **281**:17492–17500.
27. Kronenberg M (2005) Toward an understanding of NKT cell biology: progress and paradoxes. *Annu Rev Immunol* **23**:877–900.
28. Machein MR, Kullmer J, Ronicke V, Machein U, Krieg M, Damert A *et al* (1999) Differential downregulation of vascular endothelial growth factor by dexamethasone in normoxic and hypoxic rat glioma cells. *Neuropathol Appl Neurobiol* **25**:104–112.
29. Morley JE, Thomas DR, Wilson MM (2006) Cachexia: pathophysiology and clinical relevance. *Am J Clin Nutr* **83**:735–743.
30. Oliner J, Min H, Leal J, Yu D, Rao S, You E, *et al* (2004) Suppression of angiogenesis and tumor growth by selective inhibition of angiopoietin-2. *Cancer Cells* **6**:507–516.
31. Papadopoulos MC, Saadoun S, Binder DK, Manley GT, Krishna S, Verkman AS (2004) Molecular mechanisms of brain tumor edema. *Neuroscience* **129**:1011–1020.
32. Pulkkanen KJ, Yla-Herttuala S (2005) Gene therapy for malignant glioma: current clinical status. *Mol Ther* **12**:585–598.

33. Reardon DA, Wen PY (2006) Therapeutic advances in the treatment of glioblastoma: rationale and potential role of targeted agents. *Oncologist* **11**:152–164.
34. Reiss Y, Machein MR, Plate KH (2005) The role of angiopoietins during angiogenesis in gliomas. *Brain Pathol* **15**:311–317.
35. Robe PA, Nguyen-Khac M, Jolois O, Rogister B, Merville MP, Bours V (2005) Dexamethasone inhibits the HSV-tk/ganciclovir bystander effect in malignant glioma cells. *BMC Cancer* **5**:32.
36. Scherpereel A, Gentina T, Grigoriu B, Senechal S, Janin A, Tsicopoulos A *et al* (2003) Overexpression of endocan induces tumor formation. *Cancer Res* **63**:6084–6089.
37. Seino K, Motohashi S, Fujisawa T, Nakayama T, Taniguchi M (2006) Natural killer T cell-mediated antitumor immune responses and their clinical applications. *Cancer Sci* **97**:807–812.
38. Seligman AM, Shear MJ (1939) Studies in Carcinogenesis. VIII. Experimental production of brain tumors in mice with methylcholanthrene. *Am J Cancer* **37**:364–395.
39. Simmons DM, Arriza JL, Swanson LW (1989) A complete protocol for in situ hybridization of messenger RNAs in brain and other tissues with radiolabeled single-stranded RNA probes. *J Histotechnol* **12**:169–181.
40. Stupp R, Hegi ME, van den Bent MJ, Mason WP, Weller M, Mirimanoff RO, Cairncross JG (2006) Changing paradigms—an update on the multidisciplinary management of malignant glioma. *Oncologist* **11**:165–180.
41. Sur P, Sribnick EA, Patel SJ, Ray SK, Banik NL (2005) Dexamethasone decreases temozolomide-induced apoptosis in human gliobastoma T98G cells. *Glia* **50**:160–167.
42. Szatmari T, Lumniczky K, Desaknai S, Trajcevski S, Hidvegi EJ, Hamada H, Safrany G (2006) Detailed characterization of the mouse glioma 261 tumor model for experimental glioblastoma therapy. *Cancer Sci* **97**:546–553.
43. Tait CR, Jones PF (2004) Angiopoietins in tumours: the angiogenic switch. *J Pathol* **204**:1–10.
44. Terabe M, Berzofsky JA (2004) Immunoregulatory T cells in tumor immunity. *Curr Opin Immunol* **16**:157–162.
45. Thapar K, Rutka JJL (1995) Brain edema, increased intracranial pressure, vascular effects and other epiphenomena of human brain tumors. In: *Brain Tumors: An Encyclopedic Approach*. AH Kaye, ER Laws (eds), pp. 163–189. Churchill Livingstone: Edinburgh; New York.
46. Valenzuela DM, Griffiths JA, Rojas J, Aldrich TH, Jones PF, Zhou H *et al* (1999) Angiopoietins 3 and 4: diverging gene counterparts in mice and humans. *Proc Natl Acad Sci USA* **96**:1904–1909.
47. Villeneuve J, Tremblay P, Vallieres L (2005) Tumor necrosis factor reduces brain tumor growth by enhancing macrophage recruitment and microcyst formation. *Cancer Res* **65**:3928–3936.
48. Wen PY, MacDonald L, Conrad Gigas D (2005) Managment of non-neoplastic problems in brain tumor patients. In: *Cancer of the Nervous System*. PM Black, JS Loeffler (eds), pp. 243–254. Lippincott Williams & Wilkins: Philadelphia.
49. Wheeler CJ, Black KL, Liu G, Ying H, Yu JS, Zhang W, Lee PK (2003) Thymic CD8+ T cell production strongly influences tumor antigen recognition and age-dependent glioma mortality. *J Immunol* **171**:4927–4933.
50. Zagzag D, Amirnovin R, Greco MA, Yee H, Holash J, Wiegand SJ *et al* (2000) Vascular apoptosis and involution in gliomas precede neovascularization: a novel concept for glioma growth and angiogenesis. *Lab Invest* **80**:837–849.

SUPPLEMENTARY MATERIAL

The following supplementary material is available for this article:

Table S1. cDNAs used for *in situ* hybridization.

Table S2. Primers used for qRT-PCR.

Table S3. Genes identified as being modulated in GL261 cells after a 24-h incubation with 1 μg/mL dexamethasone (Dex). For concision, only one probe set per gene is shown. A negative ratio indicates that the gene is down-regulated.

Table S4. Genes identified as being modulated in bEnd3 cells after a 24-h incubation with 1 μg/mL dexamethasone (Dex). For concision, only one probe set per gene is shown. A negative ratio indicates that the gene is down-regulated. Genes classified as "extracellular" in the Gene Ontology database are labeled with an "x."

This material is available as part of the online article from: http://www.blackwellsynergy.com

Please note: Blackwell Publishing is not responsible for the content or functionality of any supplementary materials supplied by the authors. Any queries (other than missing material) should be directed to the corresponding author for the article.